

A NUMERICAL STUDY OF THE BOUNDARY LAYER DYNAMICS INSIDE ARIZONA'S METEOR CRATER

MICHAEL T. KIEFER* AND SHIYUAN ZHONG
Michigan State University, East Lansing, Michigan

1. INTRODUCTION

An improved understanding of the physical processes governing the evolution of cold-air pools inside mountain basins was a primary motivation for the METCRAX experiment conducted during October 2006 within Arizona's Meteor Crater near Winslow, Arizona (Whiteman et al., 2008). While other field studies have contributed to our understanding of stable boundary layer structure and evolution in valleys and basins (e.g., Whiteman et al., 1999; Clements et al., 2003; Steinacker et al., 2007), the METCRAX experiment was unique in terms of the idealized nature of the study area. Meteor Crater, being symmetrical in shape and exhibiting uniform slope and sidewall heights without gaps, made it an ideal site for examining boundary layer growth and evolution. The crater, formed approximately 50,000 years ago by a meteorite impact, is approximately 165 m deep and 1200 m in diameter at rim level. The rim of the crater rises approximately 50 m above the surrounding plain of the Colorado Plateau and is unbroken by large saddles or passes.

Analysis of the METCRAX data as reported in previous studies (Whiteman et al., 2008; Yao and Zhong, 2009) has revealed several aspects of the crater atmosphere for which the physical mechanisms are not well understood. First, a quasi-steady three-layer thermal structure was observed within the crater during quietest nights (including the night of 22-23 October 2006), consisting of a strong surface inversion, an overlying nearly isothermal layer, and a secondary inversion near the top of the crater (Fig. 1). Such a structure had not been observed in prior studies of nocturnal boundary layer structures in closed basins (e.g., Clements et al., 2003). Second, a horizontally homogeneous state was observed away from the crater floor and the sidewalls, as evidenced by the nearly identical profiles measured at the three sites spanning the crater (Fig. 1). Other aspects of the crater have also been identified, including asym-

metry in the inflow on the western and eastern sidewalls of the crater (Kossmann et al., 2009), and a tendency for air flowing toward the crater to pass over rather than descend into the basin (Whiteman et al., 2008; Kossmann et al., 2009). Recent observational and modeling studies have also considered the effect of the rim on the atmosphere inside the crater basin, with some studies suggesting an important link between the rim and the unique properties of the nocturnal crater atmosphere (Kossmann et al., 2009; Whiteman et al., 2010). The primary goal of this study is examine the nocturnal basin evolution and evaluate the influence of the rim on the evolution via a series of numerical simulations.

2. METHOD

The numerical model utilized for this study is the Advanced Regional Prediction System (ARPS) Version 5.2.7 (Xue et al., 2000, 2003). ARPS is a three-dimensional, compressible, nonhydrostatic atmospheric modeling system with a terrain-following coordinate system. A 1.5-order subgrid-scale turbulence closure scheme with a prognostic equation for the turbulent kinetic energy is utilized, as well as a land surface and vegetation model based on Noilhan and Planton (1989) and Pleim and Xiu (1995) and radiation physics following Chou (1990, 1992) and Chou and Suarez (1994). Effects of topographic shading on radiative fluxes are accounted for as in Colette et al. (2003). Fourth-order accurate finite differencing of the advection terms is used in both the vertical and horizontal directions, while the upper boundary condition for all simulations is a sponge layer from $z = 10$ km to the model top at $z = 12$ km.

In this study, we utilize a combination of 3D real data and 2D idealized simulations to examine crater atmosphere processes. For the real data simulations, a series of one-way nested simulations are executed, spanning from 9-km to 50-m horizontal grid spacing with an approximately 1:3 nesting ratio with each simulation initialized at 0500 MST 22 October 2006. North American Regional Reanalysis data (NARR) (Mesinger et al., 2006) is used to specify both initial and boundary conditions for the outermost grid. Land use and terrain data are input from the U.S. Geological Survey (USGS) 1-km

*Corresponding author address: Michael Kiefer, Department of Geography, Michigan State University, 116 Geography Building, East Lansing, MI 48823.
E-mail: mtkiefer@msu.edu

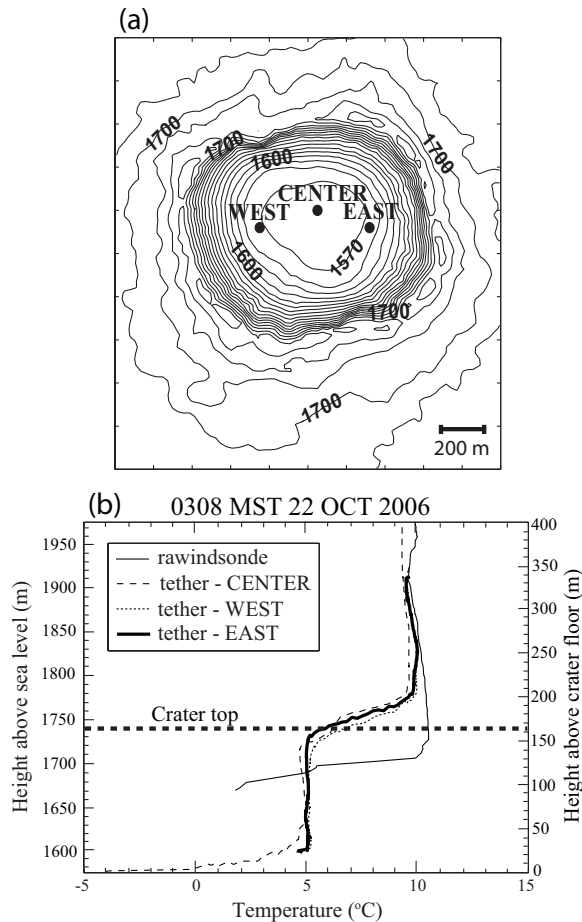


Figure 1: (a) Topographic map of Arizona's Meteor Crater with locations of tethersonde sites overlaid. (b) Coincident temperature soundings made from the west, center, and east tethersondes inside the crater and the rawinsonde outside the crater at 0308 MST 23 Oct 2006. For reference, the rawinsonde site is located approximately 5 km north-northwest of the crater. Elevation of crater rim is indicated by horizontal dashed line.

and 100-m datasets, respectively. The outermost grid contains most of Arizona, as well as portions of New Mexico, Colorado, Utah, and Nevada, with the innermost grid consisting of a 25-km² area centered on the crater (Fig. 2). The model terrain does not feature a rim (see Fig. 2c) due to the relatively coarse topographic dataset used for this study. Stretching is applied along the vertical axis with a minimum vertical grid spacing of 2.5 m near the surface in the 50-m grid spacing innermost grid. The grid is gradually stretched to 300 m at the model top near 12 km above mean sea level (MSL).

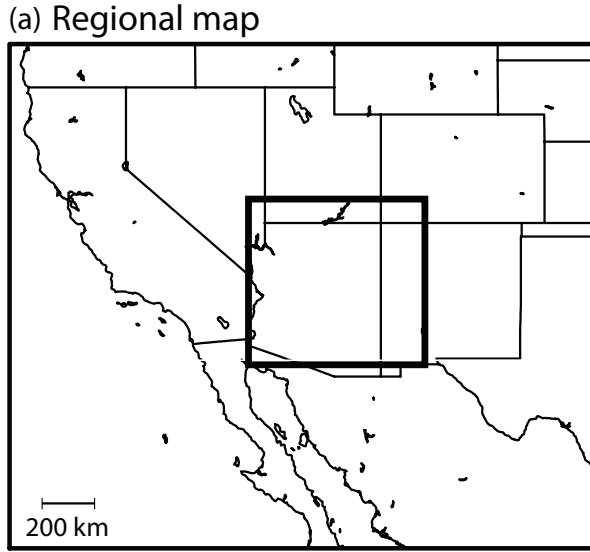
The 2D idealized simulations are initialized with a 17 MST 22 October sounding upstream of the crater, obtained from the innermost grid real data simulation, and run for 12 hours. Horizontal and vertical grid spacing of 30 m and 2.5 m, respectively, allows the model to resolve the crater rim; simulations with and without the rim are then examined to evaluate the role of the rim in cold-air pool processes. Unless otherwise specified, model parameters (e.g. subgrid-scale turbulence parameterization) are identical in the real data and idealized simulations.

3. RESULTS

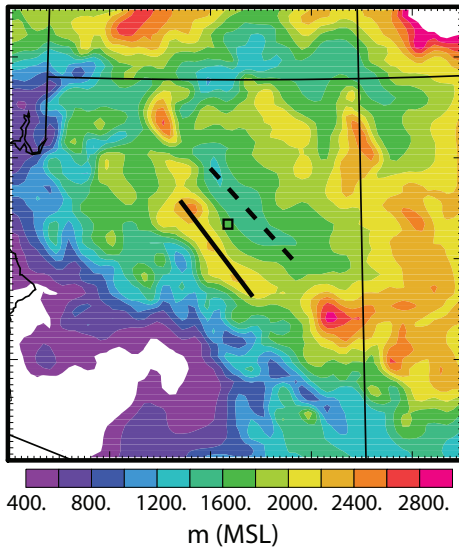
a. 3D Real Data Simulations

Before proceeding to examine the evolution of the model crater atmosphere, it is important to assess the ability of the 3D model simulation to reproduce the observed crater characteristics. Regarding the three-layer thermal structure discussed earlier, it is apparent from Fig. 3 that the model is able to reproduce the phenomenon. One can see that two inversions are present in the temperature profile at 2000 MST 22 October (hereafter, 2000 MST), one spanning the lowest 10-15 m of the crater, and the second beginning near the height of the model crater top and extending approximately 50 m upward. The layer between the two inversions exhibits much weaker potential temperature lapse rates and is, in fact, near isothermal. Accounting for the cold bias in the initial condition and the shallow crater depth, the model does reasonably capture the three-layer structure. Note that although the three-layer structure is also present later at 2300 and 0200 MST (not shown), periods of time do exist during the night when the isothermal layer is replaced with a somewhat more stable layer.

In order to better examine the evolution of the model crater atmosphere, vertical cross sections of potential temperature are presented in Fig. 4. During the first 1-2 hours following astronomical sunset, the potential temperature of the drainage flow approaching the crater is colder than the potential temperature at the same elevation inside the crater (Fig. 4a). Thus, negatively buoyant air pours into the crater, contributing to the cold pool



(b) Coarse grid



(c) Finest grid

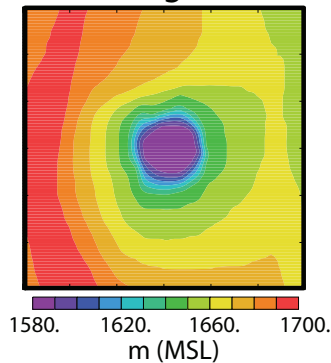


Figure 2: Summary of grid nesting strategy: (a) political map of the southwestern U.S. with outermost grid domain outlined, and surface elevation maps of the (b) outermost and (c) innermost grid domains. Axes of principal topographic features in the vicinity of the crater are marked in panel (b): Mogollon Rim - solid line; Little Colorado River Valley - dashed line.

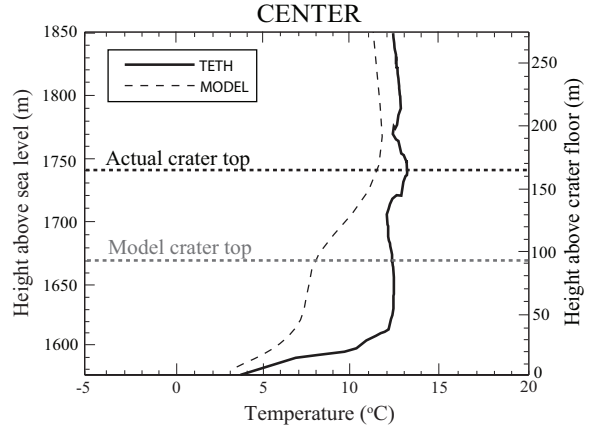


Figure 3: Vertical profiles of temperature (K) at 2000 MST 22 Oct 2006 (0300 UTC 23 Oct 2006), valid in crater center. TETH profiles corresponds to tetheredsonde observations from the METCRAX experiment and MODEL refers to the ARPS simulation. Elevation of actual and model crater top indicated by horizontal black and gray dashed lines, respectively; differences in crater top elevation result from the relatively coarse (100 m) resolution of the terrain dataset.

at the basin floor, while compensating vertical advection cools the crater atmosphere away from the floor and sidewalls. It is worth noting that during the period 1700-1900 MST, when intrusion of air into the crater is most robust, inflow occurs predominately along the western sidewall (i.e., the inflow is asymmetric).

By 2000 MST, the crater atmosphere has cooled to the point where approaching air is neutrally buoyant with respect to the air at the same elevation inside the crater, and the incoming air sweeps across the top of the basin (Fig. 4b). Although differences between the atmosphere inside the crater and over the surrounding plain are initially small (Fig. 4a), the crater atmosphere evolves into a three-layer structure by 2000 MST (Fig. 4b). It is also important to note the horizontally homogeneous nature of the crater atmosphere at 2000 MST (Fig. 4b) and especially at 2200 MST (Fig. 4c). Apart from the area immediately adjacent to the sidewalls, the vertical thermal structure within the crater is largely independent of location.

b. 2D Idealized Simulations

We next present results from a series of 2D sensitivity tests using an idealized terrain dataset. The lack of a rim surrounding the crater in the 3D terrain dataset raises an important question: are the results presented thus far applicable to a crater with a rim? Thus, our interest here lies not in reproducing all details of the crater atmosphere observed during IOP 5, but in examining the impact, if any, of the rim on the evolution of the nocturnal boundary layer inside Meteor Crater.

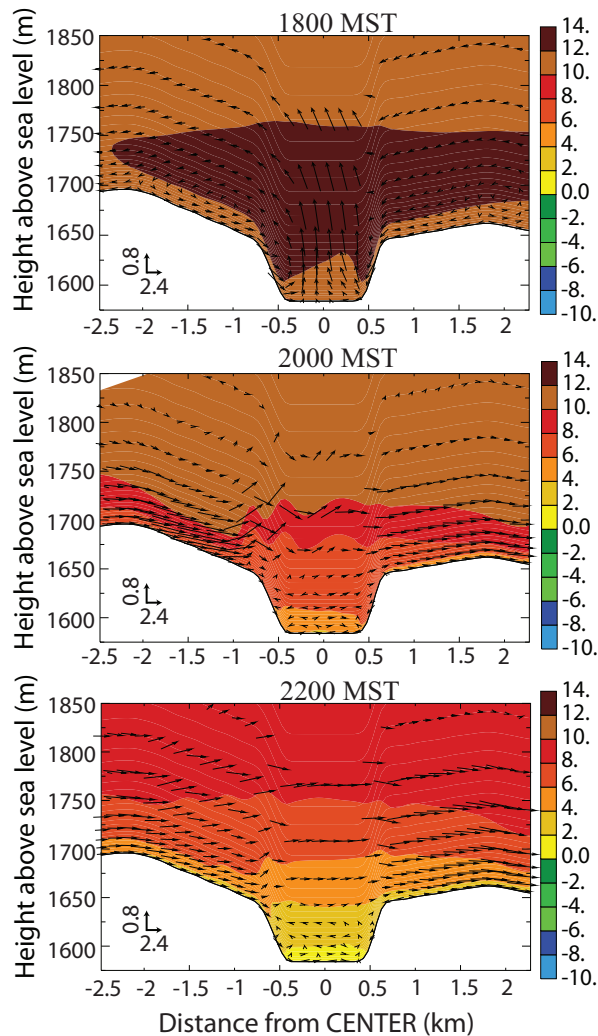


Figure 4: Vertical cross sections of temperature (shaded and contoured; $^{\circ}\text{C}$) and 3D wind vectors projected onto the x - z plane (m s^{-1}) for (a) 1800 MST, (b) 2000 MST, and (c) 2200 MST 22 Oct 2006. Cross section is oriented west-east through the center of crater at point CENTER. The crater extends 0.6 km to the west and east of the position marked 0 on the x -axis; note that the surrounding plains exhibit much more gently sloping terrain ($\sim 3\%$ slope). The vector key is provided in the lower-left corner of each panel.

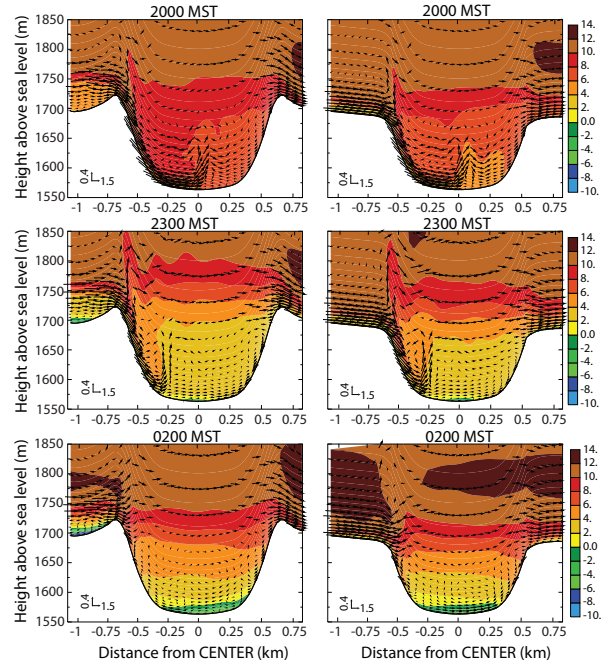


Figure 5: Vertical Cross-sections of temperature ($^{\circ}\text{C}$) and wind vectors (m s^{-1}) in west-east oriented plane through crater center, for simulations (left) with rim and (right) without rim.

As can be seen in Fig. 5, the evolution of the crater atmosphere is identical in simulations with and without a rim, although changes are delayed by 20-25 minutes in the simulation with a rim. The evolution outlined in the prior section, that of cold air intrusion, cold-pool deepening, and eventual deflection of air over the top of the crater basin, occurs in both simulations. Caution must be exercised, however, in generalizing this finding and applying it to non-quietest overnight periods. In cases with stronger synoptic-scale flow, the rim may play an important role in the nocturnal evolution of the crater atmosphere, predominately through turbulence production.

4. CONCLUSIONS

Utilizing a combination of 3D real data and 2D idealized simulations, this study has examined the evolution of the nocturnal boundary layer observed within Arizona's Meteor Crater during the METCRAX field campaign IOP 5 (22-23 October 2006). The simulated crater atmosphere evolution can be summarized as follows. During early evening, the intrusion of cold air from outside of crater dominates cold-air pool development. Late in the evening, cooling of the crater atmosphere renders incoming air neutrally buoyant; regional-scale drainage flow is subsequently deflected above the crater basin. During the late evening, in-situ cooling dominates cold-air pool

evolution. A series of 2D sensitivity experiments show that this evolution is not dependent on the presence of a rim, although the rim was shown to delay changes by 20-25 minutes compared to the no-rim simulation.

In spite of the stated limitations of this study, results presented in this paper represent an important step in improving our understanding of nocturnal boundary layer evolution in closed basins. This study also provides insight into how airflow outside of a closed basin can impact the boundary layer structure inside. Ongoing work involves performing additional idealized simulations of the atmosphere in Meteor Crater in order to examine the impact of crater geometry and upstream conditions on the nocturnal boundary layer structure. More generally, analysis of METCRAX field observations and model results are expected to yield large advances in our knowledge of the boundary layer in complex terrain.

ACKNOWLEDGMENTS

We wish to thank the National Center for Atmospheric Research (NCAR) staff for providing equipment, field support and data processing, and the Barringer Crater Corporation and Meteor Crater Enterprises, Inc. for providing crater access, during the METCRAX experiment. This research was supported by the U.S. National Science Foundation Physical and Dynamic Meteorology Division (A. Detwiler, Program Manager) through Grant 0837860. Any opinions, findings, and conclusions or recommendations expressed are those of the authors and do not necessarily reflect the views of the National Science Foundation. All simulations were performed on the NCAR supercomputer *Bluefire*, managed and operated by the Computational and Information Systems Laboratory (CISL)

REFERENCES

- Chou, M.-D., 1990: Parameterization for the absorption of solar radiation by O₂ and CO₂ with application to climate studies. *J. Climate*, **3**, 209–217.
- Chou, M.-D., 1992: A solar radiation model for climate studies. *J. Atmos. Sci.*, **49**, 762–772.
- Chou, M.-D., and M. J. Suarez, 1994: An efficient thermal infrared radiation parameterization for use in general circulation models. NASA Tech. Memo 104606, 85 pp. [Available from NASA Center for Aerospace Information, 800 Elkridge Landing Road, Linthicum Heights, MD 21090-2934]
- Clements, C. B., C. D. Whiteman, and J. D. Horel, 2003: Cold-air-pool structure and evolution in a mountain basin: Peter Sinks, Utah. *J. Appl. Meteor.*, **42**, 752–768.
- Colette, A. G., F. Katopodes Chow, and R. L. Street, 2003: A numerical study of inversion-layer breakup and the effects of topographic shading in idealized valleys. *J. Appl. Meteor.*, **42**, 1255–1272.
- Kossmann, M., S. W. Hoch, C. D. Whiteman, and U. Sievers, 2009: Modeling of nocturnal drainage winds at meteor crater, arizona using KLAM.21. Preprints, *30th International Conference on Alpine Meteorology*, Rastatt, Germany, 182–183.
- Mesinger, F., G. DiMego, E. Kalnay, K. Mitchell, P. C. Shafran, W. Ebisuzaki, D. Jovic, J. Woollen, E. Rogers, E. H. Berbery, M. B. Ek, Y. Fan, R. Grumbine, W. Higgins, H. Li, Y. Lin, G. Manikin, D. Parrish, and W. Shi, 2006: North American Regional Reanalysis. *Bull. Amer. Meteor. Soc.*, **87**, 343–360.
- Noilhan, J., and S. Planton, 1989: A simple parameterization of land surface processes for meteorological models. *Mon. Wea. Rev.*, **117**, 536–549.
- Pleim, J. E., and A. Xiu, 1995: Development and testing of a surface flux and planetary boundary layer model for application in mesoscale models. *J. Appl. Meteor.*, **34**, 16–32.
- Steinacker, R., C. D. Whiteman, M. Doringner, E. Mursch-Radlgruber, K. Baumann, S. Eisenbach, A. M. Holzer, and B. Pospichal, 2007: A sinkhole field experiment in the Eastern Alps. *Bull. Amer. Meteor. Soc.*, **88**, 701–716.
- Whiteman, C. D., S. W. Hoch, M. Lehner, and T. Haiden, 2010: Nocturnal cold air intrusions into a closed basin: Observational evidence and conceptual model. *J. Appl. Meteor. Climatol.*, **999**, In Press.
- Whiteman, C. D., A. Muschinski, S. Zhong, D. Fritts, S. W. Hoch, M. Hahnenberger, W. Yao, V. Hohreiter, M. Behn, Y. Cheon, C. B. Clements, T. W. Horst, W. O. J. Brown, and S. P. Oncley, 2008: Metcrax 2006 - Meteorological experiments in Arizona's Meteor Crater. *Bull. Amer. Meteor. Soc.*, **89**, 1665–1680.
- Whiteman, C. D., S. Zhong, and X. Bian, 1999: Wintertime boundary layer structure in the Grand Canyon. *J. Appl. Meteor.*, **38**, 1084–1102.
- Xue, M., K. K. Droegemeier, and V. Wong, 2000: The Advanced Regional Prediction System (ARPS) – A multi-scale nonhydrostatic atmosphere simulation and prediction model. Part I: Model dynamics and verification. *Meteor. Atmos. Phys.*, **75**, 463–485.
- Xue, M., D. Wang, J. Gao, K. Brewster, and K. K. Droegemeier, 2003: The Advanced Regional Prediction System (ARPS), storm-scale numerical weather prediction and data assimilation. *Meteor. Atmos. Phys.*, **82**, 139–170.
- Yao, W., and S. Zhong, 2009: Nocturnal temperature inversions in a small, enclosed basin and their relationship to ambient atmospheric conditions. *Meteor. Atmos. Phys.*, **103**, 195–210.